Nucleus-Nucleus Potential inside the Strong-Absorption Radius from $^{16}O + ^{12}C$ Elastic Scattering at 94 MeV/u

P. Roussel, N. Alamanos, F. Auger, J. Barrette, B. Berthier, B. Fernandez, and L. Papineau
Département de Physique Nucléaire/Basses Energies, Centre d'Etudes Nucléaires de Saclay, F-91191 Gif-sur-Yvette Cedex, France

and

H. Doubre and W. Mittig
Grand Accelerateur National d'Ions Lourdes, F-14021 Caen Cedex, France
(Received 18 February 1985)

The elastic-scattering angular distribution for the reaction of ^{16}O on ^{12}C has been measured at $E_{lab} = 1503$ MeV. Optical-model analysis shows that the data determine the nuclear potential between 4 and 6 fm, i.e., well inside the strong-absorption radius. Above $\theta_{c.m.} = 3°$, the main contribution to the cross section comes from negative-angle scattering; however, the measured angular distribution is not sensitive to the position of the nuclear rainbow.

PACS numbers: 21.30.+y, 25.70.Cd

The study of the nucleus-nucleus potential in the intermediate energy range (10–100 MeV/u) is interesting since in this region of transition, as the energy increases, the potential dominated by nucleon correlation and antisymmetrization effects should give way to potentials determined by free nucleon-nucleon scattering. Theoretical calculations predict that this results in a strong energy dependence of the nuclear potential particularly in a region corresponding to large overlap of the nuclei.[1,2] A sensitive test of these models should come from the study of heavy-ion elastic scattering. In a first step it is, however, important to understand better the properties of the nuclear interaction by elastic angular distributions at these energies. For that purpose we have studied the scattering of ^{16}O on ^{12}C at 94 MeV/u.

The experiment was performed with the ^{16}O beam from the GANIL accelerator. The experimental technique is similar to that used to measure the elastic scattering of ^{40}Ar at 44 MeV/u.[3] Focusing of the beam on axis near the detection system resulted in an angular uncertainty of less than 0.02° and an angular dispersion of 0.05°. The energy resolution was about 2 MeV so that at all angles the elastic peak was completely separated from inelastic events. The absolute normalization was deduced from the target thickness and the integrated incident charge. It is believed to be precise to ±5%. The measured angular distribution is presented in Fig. 1.

The data were first analyzed in the framework of the optical model on the assumption of a six-parameter Woods-Saxon (WS) potential. The calculations were done with the code ECIS.[4] The depth of the real potential was scanned in steps of 10 MeV and for each value of the depth a search was done on the five remaining parameters. The resulting parameters for some of the potentials are given in Table I. The depth of 80 MeV (solid line in Fig. 1) is very close to the value which provides the best fit to the data (based on minimum χ^2). The two extreme values presented in the table give the limits where a good description of the data is obtained. The calculated angular distributions for these potentials are also presented in Fig. 1.

The ratio of the different real potentials that fit the data to that of 80 MeV is shown in Fig. 2(a) as a function of the radius. When the depth of the potential is varied, one clearly observes that the other parameters readjust themselves so as to give nearly the same po-

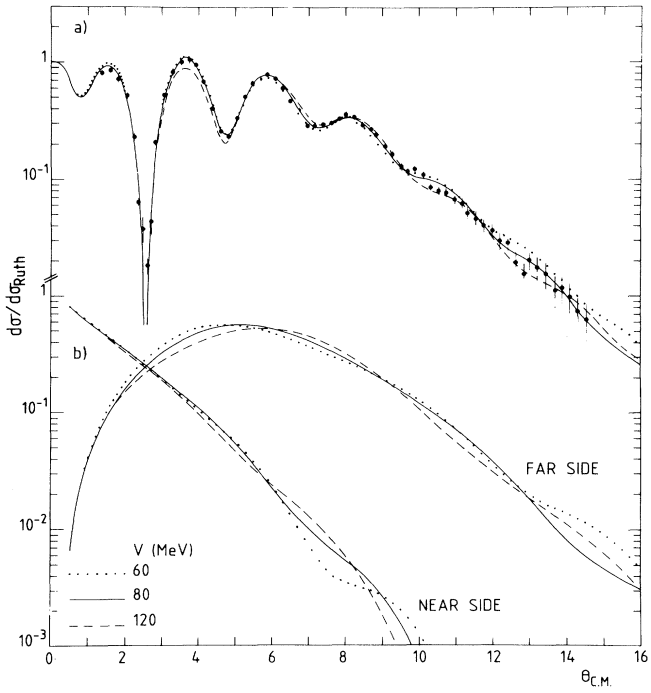

FIG. 1. (a) Elastic-scattering angular distribution for ^{16}O on ^{12}C at $E_{lab} = 1503$ MeV. The curves are optical-model calculations. (b) Far-side/near-side decomposition of the calculated angular distributions for Woods-Saxon potentials.

TABLE I. Potential parameters obtained from the analysis of the $^{16}O+^{12}C$ elastic-scattering data.

V (MeV)	r_r (fm)	a_r (fm)	W (MeV)	r_i (fm)	a_i (fm)	χ^2
			WS			
60	0.962	0.723	24.1	1.000	0.948	2.20
70	0.919	0.760	27.6	1.000	0.838	1.37
80	0.881	0.784	28.8	1.008	0.800	1.07
100	0.812	0.836	30.6	1.011	0.758	2.02
120	0.748	0.893	27.4	1.050	0.723	3.70
			$(WS)^2$			
60	1.119	0.994	72.6	0.767	2.20	1.85
80	1.047	1.136	50.6	0.975	1.675	1.55
100	0.993	1.248	50.3	1.013	1.454	1.71
120	0.946	1.325	51.5	1.032	1.319	1.95
140	0.910	1.425	62.2	1.046	1.043	2.15
			Folding			
	Normalization =0.67		39.3[a]	1.144	1.035	8.53

[a]Parameters for a squared Woods-Saxon form factor.

tential value between 4 and 6 fm. This results in all the potentials having not only the same average value but also the same first derivative in the middle of the sensitive region.

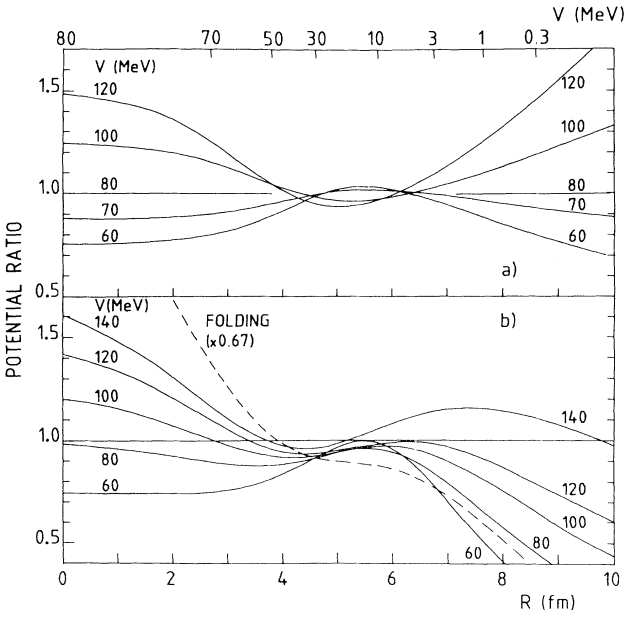

FIG. 2. (a) Ratios of the Woods-Saxon potentials to the 80-MeV-deep potential. (b) Ratio of the squared Woods-Saxon potentials (solid lines) and of the normalized folded potential (dashed line) to the 80-MeV-deep Woods-Saxon potential.

To verify that this result is not due to the functional form of the potentials (i.e., Woods-Saxon), we performed a similar analysis using a squared Woods-Saxon form factor [$(WS)^2$] for both the real and imaginary parts of the interaction. This type of potential has been successful in the analysis of light-ion angular distributions and their radial dependence is closer to that of potentials obtained by the folding model.[5] The parameters for some of the potentials which give a good fit to the data are given in the table. The fits are qualitatively very similar to that obtained with a standard Woods-Saxon potential.

The ratio of the $(WS)^2$ potentials to the 80-MeV-deep WS potential is presented in Fig. 2(b) as a function of the radius. Once more, we observe that all the potentials have similar values in the region between 4 and 6 fm and that they have nearly the same value as the (WS) potentials. This last analysis demonstrates also that the crossovers observed in Fig. 2(a) near 4.4 and 6.1 fm are due to the specific form factor used and should not be interpreted as some critical radii where the potential would be better determined.

Finally the data were fitted using a double-folded potential. For the nuclear densities we used the charge densities obtained from electron-scattering data[6] after unfolding of the nucleon charge density. This procedure gives potentials identical to those of Stokstad *et al.*[7] for $^{12}C+^{12}C$ and of Kobos *et al.*[8] for $^{16}O+^{28}Si$ where particle wave functions were used to generate the nuclear densities. For the nucleon-nucleon interaction we took the M3Y spin- and isospin-independent interaction[9] including the energy-dependent zero-range term which simulates the effect of knockon exchange. The resulting potential is 265

MeV deep at $r=0$ and should represent the free nucleon-nucleon contribution to the interaction potential. As usual, to fit the data we have allowed a renormalization of the real potential whereas the imaginary potential was assumed of a squared Woods-Saxon form with three free parameters. The folded potential has to be multiplied by a factor of 0.67 to fit the data (see Table I). Such a reduction is similar to that observed for other systems at high energy.[10-12]

The ratio of the renormalized folded potential to the best-fit Woods-Saxon potential is presented in Fig. 2(b) (dashed line). Even after renormalization the folded potential does not provide a very good description of the data (see Table I). This is probably because the potential is still too strong in the interior. Nevertheless, the normalization factor giving the best fit corresponds to a potential which is close to the others in the sensitive region, near 5 fm.

From the above analysis we can conclude that the data are very sensitive to the value of the nuclear interaction in the region between 4 and 6 fm. Variations of less than $\pm 10\%$ are observed for all the potentials which reproduce the measured angular distribution. The limits of this sensitive region should be compared with the strong-absorption radius which is 6.0 fm and with the sum of the half-density radii, i.e., 5.0 fm. Our result demonstrates clearly that high-energy elastic scattering probes the nuclear interaction over a broad region corresponding to an important overlap of the nuclei. Sensitivity to the potential inside the strong-absorption radius has also been observed for the system $^{12}C+^{12}C$ at high energy by a notch test.[10,11] The present analysis, is, however, more extensive and gives some estimate of the domain where, and the precision with which, the potential is determined.

Coupling to inelastic channels has not been included in the above calculations. Only a coupled-channels analysis including the first 2^+ state in ^{12}C has been performed and has resulted in a potential which is within a few percent equal in the sensitive region to the potential obtained by fitting the elastic angular distribution alone.

It is interesting to note that at 5 fm the present normalization factor of the folded potential (i.e., 0.67) is very close to the ratio 0.69 between the theoretical potential for $^{12}C+^{12}C$ at 86 MeV/u calculated considering a two Fermi sphere nuclear matter picture in a local density approximation[2] and the folded potential for this system. This normalization factor should change with energy since in the present domain the energy dependence of the M3Y interaction is very different from that predicted by the model of Ref. 2. The amount of precise data is, at present, not sufficient to test this prediction.

It has been suggested[13,14] that the observation of a nuclear rainbow is determinant to get the nuclear interaction inside the nucleus. For that reason the possible manifestation of a rainbow in the scattering of heavy nuclei at high energy is presently the subject of much discussion. It was argued that the presence of an exponential falloff at large angles in the scattering of $^{12}C+^{12}C$ at 25 MeV/u (Ref. 10) and 86 MeV/u (Brandan[11] and Buenerd *et al.*[15]) is the signature of such a rainbow. More recently, however, this falloff was attributed to the flux leaking in the shadow region produced by the strong absorption of the scattering amplitude at negative angle.[16,17]

The sensitivity of the present data to the nuclear rainbow can be inferred from the deflection functions presented in Fig. 3(a). They all present a nuclear rainbow in a region where the absorption is not complete. However, the behavior of these functions as the depth of the potential varies demonstrates clearly that the rainbow angle and its angular momentum are not determined by the main features of the data. This is in agreement with the location of the sensitive region which, as visualized in Fig. 3 by the distance of closest approach R_{min}, does not extend sufficiently into the interior to include the rainbow in most cases.

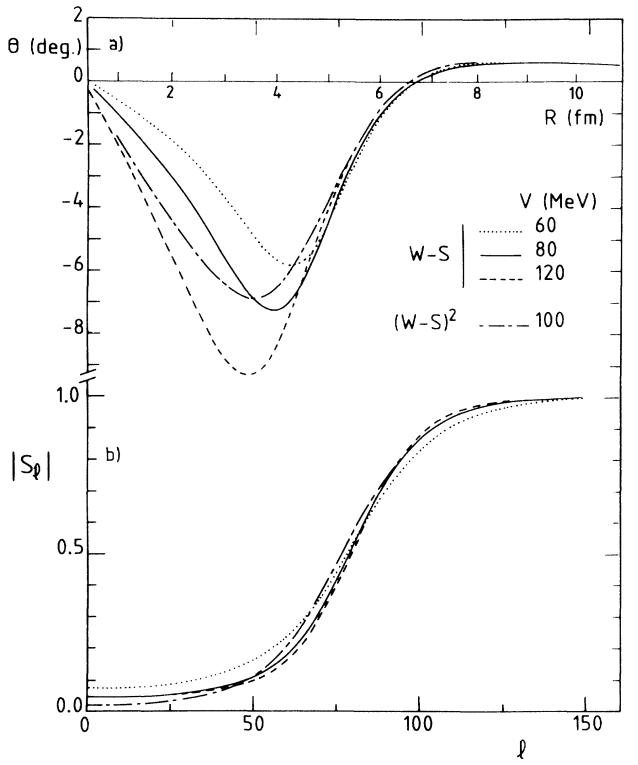

FIG. 3. (a) Classical deflection functions for some of the potentials which fit the data. The upper scale gives the corresponding distance of closest approach for the 80-MeV-deep Woods-Saxon potential. (b) Corresponding amplitude of the S matrix.

It was suggested in Ref. 17 that the signature of a nuclear rainbow should be the presence of Airy beats below the rainbow angle due to the interference between the negative branches of the deflection function. At the present energy there would be no such signature (even without absorption). The rainbow is at too small an angle as compared to the angular frequency of the Airy beats for an interference pattern to develop.

This conclusion is confirmed if one decomposes the optical-model amplitude into contributions from positive-angle (near-side) and negative-angle (far-side) scattering. Such a decomposition for the angular distributions calculated with the 60-, 80-, and 120-MeV-deep Woods-Saxon potentials following the method suggested by Fuller[18] is presented in Fig. 1(b). All potentials which fit the data result in a similar decomposition. The far-side amplitude is smooth and the oscillations of the angular distribution come from the interference between the positive-angle and negative-angle contributions. At angles larger than 4° negative-angle scattering largely dominates. It is in this relatively structureless tail that a signature for a possible nuclear rainbow has to be searched for.

In conclusion, even if the nuclear rainbow cannot be localized, heavy-ion elastic angular distribution at high energy determines precisely the nuclear interaction in a region corresponding to a large overlap of the nuclei. This should provide a severe test of the theoretical models which predict the energy dependence of the ion-ion potential.

[1]R. Sartor and Fl. Stancu, Nucl. Phys. **A404**, 392 (1983).
[2]A. Faessler *et al.*, Nucl. Phys. **A428**, 271 C (1984).
[3]N. Alamanos *et al.*, Phys. Lett. **137B**, 37 (1984).
[4]J. Raynal, Phys. Rev. C **23**, 2571 (1981).
[5]F. Michel and R. Vanderpoorten, Phys. Rev. C **16**, 142 (1977).
[6]C. W. de Jager, M. de Vries, and C. de Vries, At. Data Nucl. Data Tables **14**, 479 (1974).
[7]R. G. Stokstad *et al.*, Phys. Rev. C **20**, 655 (1979).
[8]A. M. Kobos *et al.*, Nucl. Phys. **A395**, 248 (1983).
[9]G. R. Satchler and W. G. Love, Phys. Rep. **55C**, 183 (1979).
[10]M. G. Bohlen *et al.*, Z. Phys. A **388**, 121 (1982).
[11]M. C. Brandan, Phys. Rev. Lett. **49**, 1132 (1982).
[12]M. El-Azab Farid and G. R. Satchler, to be published.
[13]D. A. Goldberg and S. M. Smith, Phys. Rev. Lett. **33**, 715 (1974).
[14]D. A. Goldberg *et al.*, Phys. Rev. C **10**, 1362 (1974).
[15]M. Buenerd *et al.*, Phys. Rev. C **26**, 1299 (1982).
[16]G. R. Satchler *et al.*, Phys. Lett. **138B**, 147 (1983).
[17]K. W. McVoy and G. R. Satchler, Nucl. Phys. **A417**, 157 (1984).
[18]R. C. Fuller, Phys. Rev. C **12**, 1561 (1975).